7-2013

Waveform Library for Chinch Bugs (Hemiptera: Heteroptera: Blissidae): Characterization of Electrical Penetration Graph Waveforms at Multiple Input Impedances

Elaine A. Backus
USDA-ARS, elaine.backus@ars.usda.gov

Murugesan Rangasamy
University of Florida

Mitchell Stamm
University of Nebraska-Lincoln

Heather J. McAuslane
University of Florida, hjmca@ufl.edu

Ron Cherry
University of Florida, rcherry@ufl.edu

Waveform Library for Chinch Bugs (Hemiptera: Heteroptera: Blissidae): Characterization of Electrical Penetration Graph Waveforms at Multiple Input Impedances

ELAINE A. BACKUS,[1,2] MURUGESAN RANGASAMY,[3,4] MITCHELL STAMM,[5] HEATHER J. MCAUSLANE,[3] AND RON CHERRY[6]

Ann. Entomol. Soc. Am. 106(4): 524–539 (2013); DOI: http://dx.doi.org/10.1603/AN13015

ABSTRACT Electrical penetration graph (EPG) monitoring has been used extensively to elucidate mechanisms of resistance in plants to insect herbivores with piercing-sucking mouthparts. Characterization of waveforms produced by insects during stylet probing is essential to the application of this technology. In the studies described herein, a four-channel Backus and Bennett AC–DC monitor was used to characterize EPG waveforms produced by adults of two economically important chinch bug species: southern chinch bug, *Blissus insularis* Barber, feeding on St. Augustinegrass, and western chinch bug, *Blissus occiduus* Barber, feeding on buffalograss. This is only the third time a heteropteran species has been recorded by using EPG; it is also the first recording of adult heteropterans, and the first of Blissidae. Probing of chinch bugs was recorded with either AC or DC applied voltage, no applied voltage, or voltage switched between AC and DC mid-recording, at input impedances ranging from 10^6 to 10^{10} Ω, plus 10^{13} Ω, to develop a waveform library. Waveforms exhibited by western and southern chinch bugs were similar, and both showed long periods of putative pathway and ingestion phases (typical of salivary sheath feeders) interspersed with shorter phases, termed transitional J wave and interruption. The J wave is suspected to be an X wave, that is, in EPG parlance, a stereotypical transition waveform that marks contact with a preferred ingestion tissue. The flexibility of using multiple input impedances with the AC–DC monitor was valuable for determining the electrical origin (resistance vs. electromotive force components) of the chinch bug waveforms. It was concluded that an input impedance of 10^7 Ω, with either DC or AC applied voltage, is optimal to detect all resistance- and electromotive force-component waveforms produced during chinch bug probing. Knowledge of electrical origins suggested hypothesized biological meanings of the waveforms, before time-intensive future correlation experiments by using histology, microscopy, and other techniques.

KEY WORDS Insecta, *Blissus*, EPG, feeding, stylet penetration

Chinch bugs within the genus *Blissus* have long been recognized as important economic pests of cultivated grasses within the United States. Two species, in particular, have gained notoriety as pests of turf and pasture grasses. The southern chinch bug, *Blissus insularis* Barber (Hemiptera: Blissidae), is the major pest of St. Augustinegrass, *Stenotaphrum secundatum* (Walter) Kuntze, a well-adapted and widely planted turfgrass species in the southern United States (Kerr 1966, Reinert and Kerr 1973). The southern chinch bug's North American geographic distribution extends from South Carolina to Florida, through the Gulf Coast states into Texas and Oklahoma, and also into California and Hawaii (Vittum et al. 1999). Its host range encompasses important turfgrasses such as Bermuda grass, *Cynodon* spp., and centipedegrass, *Eremochloa ophiuroides* (Slater 1976), but St. Augustinegrass is highly preferred (Reinert et al. 2011). A closely related species, the western chinch bug, *Blissus occiduus* Barber, is primarily an economic pest of buffalograss, *Buchloë dactyloides* (Nuttall) Englemann, a low maintenance and relatively pest-free new turfgrass for the midwestern United States (Baxendale et al. 1999). The western chinch bug has a broad host range that includes turfgrasses; agronomic crops such as wheat, barley, rye, and sorghum; and native grasses (Eickhoff et al. 2004). It is found predominantly in the

The use of trade, firm, or corporation names in this publication is for information and convenience of the reader. Such use does not constitute an official endorsement or approval by the United States Department of Agriculture or the Agricultural Research Service of any product or service to the exclusion of others that may be suitable. USDA is an equal opportunity provider and employer.

[1] Crop Diseases, Pests and Genetics Research Unit, USDA Agricultural Research Service, San Joaquin Valley Agricultural Sciences Center, 9611 South Riverbend Ave., Parlier, CA 93648.

[2] Corresponding author, e-mail: elaine.backus@ars.usda.gov.

[3] Department of Entomology and Nematology, University of Florida, Gainesville, FL 32611-0620.

[4] Present address: Dow AgroSciences, LLC, Indianapolis, IN 46268.

[5] Department of Entomology, University of Nebraska–Lincoln, Lincoln, NE 68583.

[6] Everglades Research and Education Center, University of Florida, Belle Glade, FL 33430.

0013-8746/13/0524–0539$04.00/0

western United States and Canada (Baxendale et al. 1999).

Direct feeding damage by these insects consists of discoloration of the affected tissue (Baxendale et al. 1999), with increasing areas of yellow or brown turf, and eventual death of large patches or even entire lawns or pastures (Reinert and Kerr 1973). Host plant resistance to these grass-feeding chinch bugs has been investigated as a way to manage these pests in a more environmentally friendly manner with reduced insecticide application. Categories of resistance to their respective chinch bug pests have been elucidated in several cultivars of St. Augustinegrass and buffalograss (Reinert et al. 1986; Crocker et al. 1989; Heng–Moss et al. 2002, 2003; Rangasamy et al. 2006; Eickhoff et al. 2008), but the underlying mechanisms of resistance are still unknown. The key to discovering these mechanisms will be a better understanding of chinch bug feeding.

The three *Blissus* species whose feeding effects on plants have been examined histologically are categorized as salivary sheath feeders, as sheaths of gelling saliva were found in plants fed on by chinch bugs. The sheath hardened around the chinch bug stylets as they advanced within the plant to the target tissue. Painter (1928), probably studying the common chinch bug, *Blissus leucopterus leucopterus* (Say), noted that a chinch bug feeding on corn and sorghum leaves laid down a salivary sheath as its stylets passed intracellularly on the way to the target phloem tissue. He attributed observed plant damage to the removal of photosynthate from phloem, and possibly water from the xylem, as well as clogging of the sieve tubes and tracheids with salivary sheath material (Painter 1928). Salivary sheaths of western and southern chinch bug are frequently branched as they move through the leaf tissue (Anderson et al. 2006, Rangasamy et al. 2009), and in the case of the western chinch bug, terminate primarily in the vascular tissue (Anderson et al. 2006). The target tissue of southern chinch bug stylets has not been definitively identified; however, stylets routinely pass through up to five leaf sheaths as the insects attempt to reach the youngest meristematic tissue within a leaf shoot (Rangasamy et al. 2009).

The use of electronic feeding monitors (McLean and Kinsey 1964) is the most rigorous method to investigate the feeding behavior of piercing-sucking arthropods (Walker 2000, van Helden and Tjallingii 2000). Stylet penetration behavior (or probing) of piercing-sucking insects in the order Hemiptera has been studied for more than four decades by using electronic (renamed electrical penetration graph [EPG]; Tjallingii 1985) monitoring, in which the mouthparts of a wire-tethered insect complete the electrical circuit between a plant (substrate) and an EPG monitor. Waveforms produced by changes in resistance within the circuit plus generation of voltages within the insect or plant (biopotentials) have been correlated with movement of the insect's stylets and other activities, such as salivation and ingestion (Walker 2000), rendering visible the otherwise invisible act of probing by stylet-feeding insects. Waveforms can be characterized based on frequency, amplitude, and appearance, and their electrical origin can be attributed to changes in resistance (i.e., R component of the waveform) or production of biopotentials (i.e., electromotive forces, or emf component), or a mixture of both. The biological meanings of many R versus emf electrical origins are now clearly understood (Walker 2000). For example, emf components in waveforms are caused by plant cell membrane breakages by stylets (termed intracellular punctures), or streaming potentials formed by fluid movements through capillary tubes like the food canal. R components are derived from electrical conductivity of saliva, electrical resistance to current flow from movement of valves (e.g., precibarial valve and cibarial diaphragm) in the hemipteran head, or depth of the stylets relatively to the interior of the plant, which is hypothesized to conduct higher voltages of applied signal (Walker 2000, Backus and Bennett 2009).

Certain hemipteran taxa, mostly aphids, whiteflies, and other sternorrhynchans, have been monitored primarily by using direct current (DC) monitors, where DC is applied to the feeding substrate (Tjallingii 1978) at a fixed amplifier sensitivity (or input resistance/impedance, Ri) of 10^9 Ω; output from these monitors emphasizes emf components of waveforms. Other hemipterans, in particular larger insects and those thought to be sensitive to DC, such as heteropterans and auchenorrhynchans (sharpshooter leafhoppers), have been recorded mainly with alternating current (AC) monitors (Backus 1994, Backus and Bennett 2009), formerly with a fixed Ri of 10^6 Ω; output from these monitors emphasized primarily R components. Recordings of the same species of insect with both AC and DC monitors often produced very different waveforms, confusing researchers for many years (Backus 1994). A new EPG monitor design was recently developed that allows recording of insects with either AC or DC applied signal as well as selectable Ri levels (Backus and Bennett 2009), and represents the latest refinement in the quest for a universal EPG monitor (Backus et al. 2000).

The new AC–DC four-channel monitor is similar in circuitry to the AC–DC Correlation Monitor (Backus and Bennett 2009). Signal can be applied to the plant as AC, DC, or not at all (0 V). Ri is fully selectable from 10^6 to 10^{10} Ω, plus 10^{13} Ω, permitting a researcher to match the amplifier sensitivity to the inherent resistance (Ra) of the insect, thus enabling detection of the widest array of waveforms for each species. By switching among Ri levels, one can identify waveforms composed entirely of R components (those seen at 10^6 Ω Ri) to entirely emf (those seen at 10^{13} Ω Ri). For waveforms composed of a mixture of R and emf, changes in waveform amplitude as Ri is increased or decreased reveal whether the primary component is R or emf, following the R–emf responsiveness curve. Thus, an understanding of a waveform's R and/or emf components can provide electrical evidence of the biological processes occurring inside the plant and insect during recording of these waveforms (Walker 2000, Backus and Bennett 2009).

To use EPG to investigate the mechanisms of resistance to chinch bugs in varieties of St. Augustinegrass and buffalograss, one must first characterize the waveforms produced. However, no EPG recording has been done on any *Blissus* species, or any species within the blissid family. In fact, EPG recordings of only two heteropteran species have been previously published. Feeding of first- and second-instar-nymphs of the squash bug, *Anasa tristis* (De Geer) (Hemiptera: Coreidae), a salivary sheath feeder, was recorded with an older-generation DC monitor (Bonjour et al. 1991, Cook and Neal 1999) with fixed Ri of 10^9 Ω. Waveforms from third instars of a cell rupture-feeding heteropteran, *Lygus hesperus* (Hemiptera: Miridae) (Cline and Backus 2002, Backus et al. 2007), were characterized by using an AC "Missouri monitor" (type 2.2, Backus and Bennett 1992) with fixed Ri of 10^6 Ω.

In the current study, we characterized the EPG waveforms of adults of two chinch bug species, in a third family of heteropterans to be studied by EPG (Blissidae), by using the new AC–DC four-channel monitor (Backus and Bennett 2009). Waveform families and types were described for insects feeding on plants supplied with AC, DC, or 0 V applied signal, at sequential Ri levels of 10^6 to 10^{13} Ω, providing indications of the relative amount of R and emf, and thus allowing us to hypothesize the stylet activities and biological processes represented by the characterized waveforms. Herein, we introduce a new term for EPG science: waveform library, which is defined as a collection of signal output traces, measurements, and calculations from EPG recordings of the same species at multiple input impedances.

Materials and Methods

Plants and Insects. Southern chinch bugs were collected from St. Augustinegrass lawns in Royal Palm Beach (Palm Beach County, FL) by using a modified WeedEater Barracuda blower/vacuum (Poulan/Weedeater, Shreveport, LA) (Cherry 2001). Fifth instars were separated from the debris, placed in 20-liter plastic buckets with a moist paper towel covering the bottom, and provided with fresh 'Floratam' St. Augustinegrass stolons. Insects were kept in a climate-controlled room (26°C, 40% relative humidity [RH], a photoperiod of 14:10 L:D h) at the University of Florida, Gainesville. Three- to 5-d-old adult females were used in the experiments.

Rooted single node cuttings of Floratam were grown in plastic pots (12.5 cm in diameter by 12.5 cm in depth) in a potting medium composed of equal parts fine sand (Florida Rock Inc., Jacksonville, FL) and Fafard Growing Media (Mix No. 2) (Conrad Fafard, Agawam, MA). Plants were fertilized with Osmocote Plus 15-9-12 (Scotts–Sierra Horticultural Products Company, Marysville, OH) at the rate of 5 g/kg of growing medium. Plants used as feeding substrate in the experiments were 6–8 wk old and had at least one stolon 30–40 cm in length.

Western chinch bugs were collected from buffalograss stands at the University of Nebraska–Lincoln (Lancaster County, NE) by vacuuming the soil surface with an ECHO Shred 'N' Vac (model No. ES-250; ECHO Inc., Lake Zurich, IL). Chinch bugs were sifted from samples through a 2-mm mesh screen (Heng–Moss et al. 2002) and brachypterous adults were collected with an aspirator.

Plugs of 'Prestige' buffalograss (10.6 cm in diameter by 8 cm in depth) were removed from field plots at the John Seaton Anderson Turf and Ornamental Research Facility, University of Nebraska Agricultural Research and Development Center. Buffalograss stolons were vegetatively propagated in the greenhouse in conetainers (3.8 cm in diameter by 21 cm in depth) (Stuewe & Sons Inc., Corvallis, OR) containing a potting mixture of sand–soil–peat–perlite (0.66:0.33:1:1) (Eickhoff et al. 2006). The plants were maintained in a greenhouse (25°C, 75% RH, and a photoperiod of 16:8 L:D h) under 400-W high-intensity discharge lamps. Fully established sprigs (4–5 wk after planting) were then used for EPG recordings.

Wiring and Acclimating of the Insects. Female southern chinch bugs were removed from the colony and starved for 3 h before wiring. A 12.7-μm (in diameter; sold as 0.0005 in) gold wire 1–2 cm in length (Sigmund Cohn Corp., Mt. Vernon, NY) was glued to the pronotum of the insect by using silver conductive paint (Ladd Industries, Burlington, VT). The insect was held immobile during application of the wire tether by placing its abdomen in a Pasteur pipette tip under low suction. After wiring, the insects were allowed to rest for a 1-h period on a moist paper towel to acclimate to the wire.

Western chinch bugs (sex undetermined) were starved for 17 h overnight, similarly immobilized, and then a gold wire (25 μm in diameter [sold as 0.001 in] by 1–2 cm in length) was adhered to the pronotum of the chinch bug with a small drop of silver conductive glue, composed of white glue (Elmer's Products Inc., Westerville, OH), water, and silver flake (Inframat Corp., Manchester, CT) in a 1:1:1 (vol:vol:wt) ratio.

EPG Equipment and Data Acquisition. A four-channel AC–DC EPG monitor (Backus and Bennett 2009; custom-built by the late W. H. Bennett) was used for recording the feeding behavior of four chinch bugs simultaneously on their respective host plants. Plants, insects, and the head-stage amplifiers were all placed in a Faraday cage, constructed of 1.27-cm mesh galvanized hardware metal cloth (LG Sourcing Inc., N. Wilkesboro, NC). Pots containing test plants were placed on wooden blocks to electrically isolate them from the Faraday cage. A selected stolon from each grass plant was laid down along a Plexiglas stage measuring 20 cm in length [by] 5 cm in width and fixed in place by using strips of Parafilm (Pechiney Plastic Packaging, Menasha, WI). The Plexiglas stage was held horizontally by an alligator clip connected to a "helping hand" holder (van Sickle Electronics, St. Louis, MO). The use of the horizontal stage allowed insects that had left the plant the opportunity to return by walking to the plant (unless they fell off the stage

and hung suspended from their wire tether). A 24-gauge copper wire (3 cm in length) inserted into the soil served as the plant electrode. The changes in electrical resistance as well as biopotentials during stylet probing were amplified, rectified, and digitized at 100 Hz by using a DI-720 (for southern chinch bug recordings) or DI-710 (for western chinch bug recordings) analog-to-digital board (Dataq Instruments, Akron, OH), as described by Almeida and Backus (2004), and recorded at 100 Hz by using a Dell Pentium notebook with WinDaq Pro software (Dataq).

Experimental Design: Southern Chinch Bug. In the three experiments performed, insects were attached to each of the four channels and were recorded for ≈20 h per day, under laboratory conditions and continuous light. In the first experiment, each channel (i.e., insect) was set at a different Ri level with appropriate applied signal (for both AC and DC): Ri 10^6 Ω (+30 mV), Ri 10^7 Ω (+5 mV), Ri 10^8 Ω (+5 mV), and Ri 10^9 Ω (0 mV). No negative applied signals were used. For the first half of the insects recorded, the applied signal was initially DC, then was switched to AC at 6–7 h into the recordings, and then switched to 0 mV for the last few hours. After the switch to AC, offset and gain settings were adjusted for optimum view of the waveforms (Backus and Bennett 2009). For the second half of the insects, the voltage was initially AC, then was switched to DC, and then switched again to 0 mV for the last few hours. In the second experiment, all four channels (i.e., insects) were recorded at Ri of 10^9 Ω with 2 mV applied signal. Two channels were randomly assigned to AC applied signal, and two to DC. In the third experiment, all insects were recorded at Ri of 10^{13} Ω with a 0 mV applied signal. In total, 15 chinch bugs were successfully recorded in the first experiment, five in the second, and three in the third experiment. Sample sizes of the last two experiments were small because field-collected bugs became scarcer as the unexpectedly hot and dry summer wore on.

During waveform analysis, it was found that certain aspects of waveform fine- and medium-structure, especially relative amplitude, were highly variable among insects and Ri levels, probably because of differences in wiring quality among insects (including use of silver print paint instead of the more conductive silver glue). Consequently, to test whether waveform appearances could be more stable for each Ri level if the wiring quality of each insect were improved (through use of silver glue and thicker gold wire), a second set of experiments was planned. Because southern chinch bugs were no longer available, we decided to use western chinch bugs and also to compare waveform appearances between these two closely related species.

Experimental Design: Western Chinch Bug. Waveforms were recorded in the same manner as for southern chinch bug. Two experiments were performed under laboratory conditions with continuous light. In the first, 14 insects were allowed to probe and perform all behaviors (24 h/d) until stable sustained (putative) phloem ingestion (J-I2 waveform; see later in the text) was achieved, to provide waveforms for comparison with those of southern chinch bugs. The experiment was terminated as soon as any chinch bug was no longer performing J-I2.

In the second experiment, three insects at a time were allowed to probe, until any of them achieved stable (putative) xylem ingestion (H-I2 waveform; see later in the text). At that time, the insect would not be easily disturbed by movement. Three (rather than four) insects were recorded because output from one insect per day was recorded both pre- and postrectification (Backus and Bennett 2009). Ri was then gradually switched through multiple varying levels (see next paragraph) as H-I2 continued, to observe whether and to what degree the shape of this regular continuing waveform changed with Ri level. All recordings used DC applied signal (+25 mV), so that native polarity of the output signal could be determined without offset adjustments (Backus and Bennett 2009). Thus, only gains were adjusted after each switch, for optimum display of waveforms, and then recording was continued undisturbed for 15–30 s at each Ri level, between switches. The experiment was terminated as soon as the chinch bug was no longer performing H-I2.

For 24 insects in the second experiment, EPG recordings began at Ri level of 10^7 Ω. Switches were attempted through Ri levels 10^6 ("R-only"), 10^7, 10^8, 10^9, and 10^{10} Ω (the latter four Ri levels being sensitive to varying intermediate combinations of R and emf) during each ingestion event. For an additional 27 insects, EPG recordings began with Ri 10^6 Ω. Switches made through Ri levels 10^6, 10^9, and 10^{13} Ω ("emf-only") were again attempted. For 10^{13} Ω, the applied signal was reduced to 0 mV before recording. Such a large sample size of insects (51) was necessary because it was seldom that all switches could be accomplished during a single ingestion event, or sometimes even a single insect, before the insect would be disturbed and terminate ingestion. Nonetheless, with patience, every Ri level was recorded at least six to eight times, with different insects. The exception was 10^{13} Ω, which only had two switching recordings, because of the time-consuming amount of gain reduction needed after switching from 10^{10} Ω. Amplitude of the waveforms at 10^{13} Ω often exceeded display window size ("peaked out"), because of a combination of extreme amplifier sensitivity and the highly conductive, large size of chinch bugs compared with the small size of most insects EPG-monitored previously. Gain adjustments often could not be completed before the insect became disturbed and terminated ingestion.

Waveform Terminology. Waveforms were named by following the hierarchical scheme established for *Homalodisca vitripennis* (Germar) (formerly *Homalodisca coagulata* [Say]) sharpshooters (Almeida and Backus 2004). Waveform phases describe broadly recognized types of stylet penetration activities, such as pathway versus ingestion, and can be seen at a coarse level of resolution (WinDaq compression of 25–35). When the resolution is increased (WinDaq compression of 5–12), consistent patterns of waveform shape

and amplitude can be seen; these are termed waveform families and labeled with capital letters. At a low level of compression (WinDaq compression of 2–5), the fine structure of the waveform becomes visible and waveforms within a family are designated as types and given a number. Thus, waveform family-type combination is named by alphanumeric such as A1, A2, and so on. Each uninterrupted occurrence of a certain waveform type is termed a waveform event. In the case of regular repeating waveforms such as the I waveforms (see later in the text), one stereotypical cycle of the waveform is termed an episode.

Waveform Analysis. *Comparisons of Waveform Amplitudes Across Ri Levels.* Relative amplitudes for all waveforms in southern chinch bug recordings were estimated by identifying the highest absolute-amplitude peak (measured from lowest valley to highest peak in that event) among all peaks in a waveform event, and then estimating the amplitudes of other peaks as a percentage relative to the highest peak voltage. Relative amplitudes were estimated from each event of that waveform type in at least two probes made by each of five randomly chosen southern chinch bugs (total 16 events), and amplitude estimates were expressed as rounded percentage ranges.

Comparisons of Peak and Wave Amplitudes for Waveform H-I2 Across Ri Levels. A single representative episode (termed a waveform excerpt) of waveform family H-I2 (see later in the text) was visually selected as most representative of all repetitive episodes in each H-I2 event recorded in Ri switches with western chinch bugs. Excerpts were copied into an Excel file and grouped by Ri level and insect. A single excerpt then was chosen to represent the average waveform appearance at that Ri level from all switching events, for each insect. Absolute amplitudes of the first plateau (the "peak"), as well as the third and the eighth plateaus (in the "wave"; see also further description under *Family I*), were measured, amplitude ratios for plateaus 1:3 and 1:8 were then calculated, and all ratios for all insects were statistically compared by Ri level.

Measurement of Repetition Rates. Repetition rates of regular waveforms were measured in eight randomly chosen southern chinch bugs from the first experiment (i.e., only Ri 10^7 and 10^9 Ω), and then expressed as rounded frequency ranges.

Statistical Comparison Methods. All comparisons were performed by using mixed model analysis of variance (PROC GLIMMIX, SAS Institute 2001) followed by pairwise comparisons by using Fisher least significant difference test. Data were not transformed because homogeneity was strong according to Pearson's χ^2 test. Results were considered significantly different at $\alpha = 0.05$.

Results

General Overview of Chinch Bug Waveforms and Probing Behaviors. The coarse structures of both southern and western chinch bug EPG waveforms clearly showed two main phases, termed putative pathway and ingestion phases (Table 1), as are always

Table 1. Summary of waveform characteristics for adult chinch bugs

Phase	Family	Type	Relative amplitude		Repetition rate		Voltage level at Ri 10^9 Ω	Electrical origin	Best seen at these Ri levels	Proposed biological meanings
			Ri 10^7 Ω	Ri 10^9 Ω	Ri 10^7 Ω	Ri 10^9 Ω				
Pathway	G	G1	100%	N/A[a]	Irregular	Irregular	Intracellular	All R	10^6–10^7 Ω	Secretion of thickest gelling saliva, formation of salivary flange and trunk
		G2	40–50%	N/A[a]	Irregular	Irregular	Intracellular	All R	10^6–10^7 Ω	Secretion of thickest gelling saliva, formation of salivary trunk
	H		10–50%	30–70%	Irregular + underlying regular 7–8 Hz	Irregular + underlying regular 7–9 Hz	Both intra- and extracellular	Mixed; peaks and spikes = R, irregular = R + emf	10^7–10^{10} Ω	Secretion of thinner gelling saliva, deeper penetration of stylets to vascular bundle
J wave	J		5–20%	20–40%	Rises irregular; waves 9–12 Hz	Rises irregular; waves 9–12 Hz	Intracellular	Mixed; rise and slope = R, wave = emf	10^7–10^9 Ω	Penetration of phloem sieve element; salivation, tasting, testing of salivary seal
Ingestion	I	H-I1	10–25%	70–90%	6.5–9 Hz	6.5–9 Hz	Extracellular	Mixed; peak = R, wave = emf	10^7–10^9 Ω	Active ingestion from and possible salivation into xylem tracheary element
		H-I2	10–25%	70–90%	6.5–9 Hz	6.5–9 Hz	Extracellular	Mixed; peak = R, wave = emf	10^7–10^9 Ω	Active ingestion from xylem tracheary element
	I	J-I1	2–5%	5–10%	6.5–9 Hz	6.5–9 Hz	Intracellular	Mixed; peak = R, wave = emf	10^7–10^9 Ω	Passive/active ingestion from and possible salivation into phloem sieve element
		J-I2	2–5%	5–10%	6.5–9 Hz	6.5–9 Hz	Intracellular	Mixed; peak = R, wave = emf	10^7–10^9 Ω	Passive/active ingestion from phloem sieve element
Interruption	N		10–25%	70–90%	Irregular	Irregular	Extracellular	Extracellular	10^7–10^9 Ω	Salivation into vascular cell

[a] Not applicable; waveform family G is often not distinguishable from family H at Ri levels of 10^9 Ω and higher.

seen with salivary sheath feeders. Thus, chinch bug waveforms represented distinct phases of salivary sheath formation and stylet activities while searching for vascular tissues (pathway phase), from which the insects eventually ingest sap (ingestion phase). Two shorter phases, the transitional J wave, and interruptions complete the chinch bug phases. Within waveform phase, waveform families G, H, I, and J were characterized, as well as finer-structure voltage patterns described below as individual waveform types. The waveform families occurred stereotypically in the sequence G →H →I →H →J →I in most chinch bug probes.

With the exception of waveform I (described later in the text), waveform appearances were similar between Ri levels of 10^6 and 10^7 Ω, as well as between levels 10^9 and 10^{10} Ω. Waveforms recorded at Ri 10^8 Ω were intermediate in appearance between those two, and Ri 10^{13} Ω waveforms were quite varied in appearance compared with all other Ri levels. Consequently, representative Ri levels of 10^7 and 10^9 Ω were chosen for the waveform figures, including both compressed and expanded views, to represent the evolution in waveform appearance across different Ri levels.

It was challenging to find appropriate early probe sequences that contained all waveform types for the overview figures, because the sequences had to be short enough to fit in the space available for the figures. Most H events in the G →H →I waveform sequence were typically several minutes in duration. Most recordings would have required too much compression and loss of detail to fit in the figure space. The three probes with best lengths for display came from two recordings that used different applied signal types, that is, AC for one probe at Ri 10^7 Ω, and DC for two probes (from the same insect) at Ri 10^9 Ω. Our choice of waveforms for the figures is not intended to imply that these voltage types are optimum for recordings at the respective Ri levels. On the contrary, we repeatedly found that when offset and gain settings were optimized for each Ri level (Backus and Bennett 2009), there were no consistently detectable differences in waveform appearance between AC, DC, and 0 V applied signal types, except for ingestion waveforms and Ri level 10^{13} Ω recordings, as described later. We did find, however, that waveform appearance was somewhat less variable among Ri levels when silver glue (rather than silver paint) and thicker wire were used.

Two major changes in waveform appearances occurred as Ri level was changed. First, amplitude of each waveform type increased or decreased, relative to each other, as Ri was progressively increased from 10^6 to 10^{13} Ω (described for each waveform type). Second, voltage level of all waveforms shifted. At Ri of 10^6 and 10^7 Ω, voltage levels were always monophasic, that is, waveforms floated above the 0 V baseline, with medium- and fine-structure peaks pointed positive-ward. At Ri of 10^9, 10^{10}, and 10^{13} Ω, voltage levels were biphasic, that is, within a single probe, waveforms floated either above or below the 0 V baseline; positive waveforms always had peaks pointed positive-ward, whereas negative waveforms could have peaks pointed either negative-ward or positive-ward, depending on the waveform type. At Ri of 10^8 Ω, voltage levels could be either mono- or biphasic; 10^8 Ω voltage levels were almost always consistent within each insect, suggesting that wiring quality was involved in the voltage level shift.

There also were no appreciable differences in appearance between southern and western chinch bug waveforms. Consequently, most waveform characterizations described later are taken from the recordings of southern chinch bug, but apply to western chinch bug recordings as well. Results of impedance (Ri) switching experiments with western chinch bugs are incorporated into descriptions of waveform appearance, as relates to emf versus R components. All waveform characterizations are summarized in Table 1.

Waveform Families and Types. *Family G.* At the beginning of every probe, the first waveform family, named G, was composed of a series of irregular-frequency very high-amplitude (tall) and rapid spikes or narrow peaks (Fig. 1a). G family waveforms were divided into two types, G1 and G2 (Fig. 1b). G1 was composed of extremely rapid, irregular spikes of mixed very high relative amplitude and voltage level, always at the beginning of the probe (Fig. 1a and b). G2 was composed of equally high-amplitude (but slower) plateaus and valleys with multiple (high-frequency) spikes on top of wide plateaus (Fig. 1a and b), termed "spikey plateaus." G2 spikey plateaus always followed G1 spikes, and could lead to more G1 or represent a transition to the H family (see later text). Individual G2 plateaus were often interspersed among G1 events, or followed H-I (see later text). G waveforms looked the same, regardless of whether the applied signal was AC or DC.

Both G1 and G2 were very tall at input impedance (Ri) level of 10^6 or 10^7 Ω (Fig. 1a and b), whereas they were shorter at Ri 10^8 Ω (not shown) and much shorter (often not distinguishable from H) at Ri 10^9 Ω (Fig. 2a and b and c) or 10^{10} Ω, and then disappeared entirely at Ri 10^{13} Ω (Table 1). Therefore, evidence supported that the electrical origin of waveform family G was strongly R-dominated with almost no emf. Voltage levels for G waveforms were strictly positive at Ri 10^6 and 10^7 Ω (Fig. 1a). In contrast, the base of G (when present) was negative at Ri 10^9 Ω and higher, but peaks extended positive-ward, so that the tops of peaks were above 0 V (Fig. 2a and b).

Family H. Following G1 or G2, the amplitude of the waveforms distinctly decreased. This transition marked the start of waveform family H, composed of overlying medium-structure rises and trenches that were highly variable and irregular-frequency, as well as underlying much smaller fine-structure spikes and waves (Figs. 1a and b [s and w, respectively, in the inset boxes] and 2a, b, and d). H often represented the major portion of the pathway duration in each probe. H waveforms looked the same, regardless of whether the applied signal was AC or DC, but its spikes and waves were larger with 0 V applied signal than with either AC or DC applied signal.

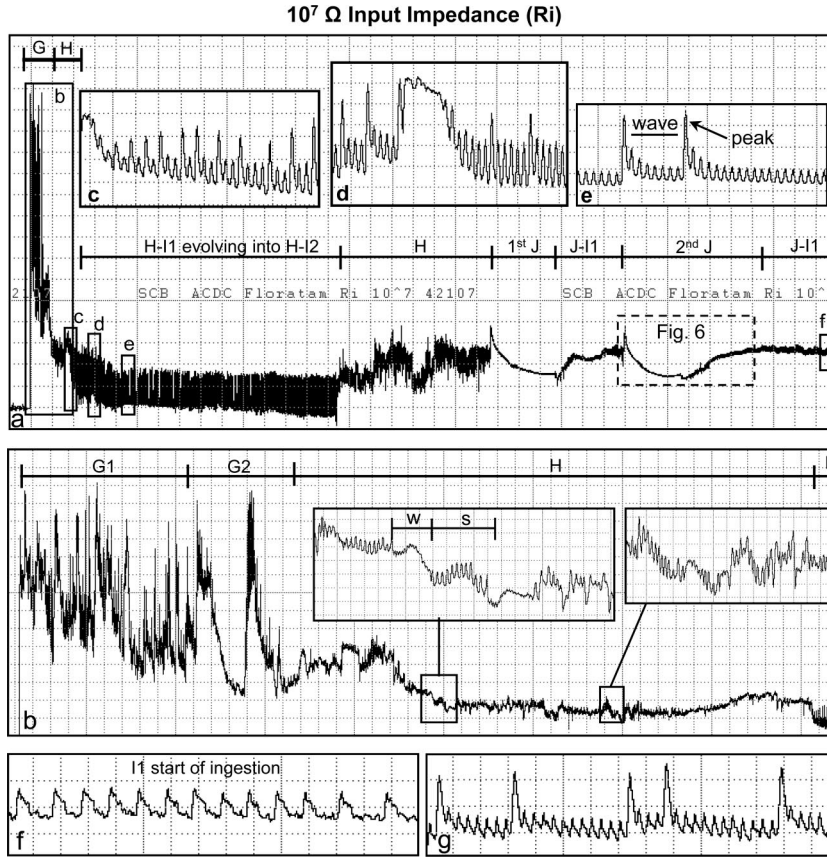

Fig. 1. Representative southern chinch bug waveforms using 5 mV AC applied signal and 10^7 Ω input impedance (Ri). (a) Compressed overview of the early part of a typical probe with pathway followed directly by putative ingestion (H-I), then further pathway (H), followed by two J waves with subsequent, evolving J-I1. Waveforms are monophasic, with 0 V baseline at bottom of view. Windaq compression 300 (60 s/vertical div.), gain 4×. Boxes b, c, d, e, and f are expanded in their respective figure parts. (b) Expanded view of box b in part a, showing G1, G2 "spikey" plateaus, and H pathway waveforms. Inset boxes show amplified (Windaq gain 16×) view, to reveal the small but distinct underlying wave (w) and 7–8 Hz-frequency spikelet burst (s). Inset compression 13 (2.6 s/vertical div.), Windaq gain 4×. (c–e) Expanded views of the same-lettered boxes in part a showing the evolution of putative ingestion waveform (H-I) appearance directly after pathway. Compression 2 (0.40 s/vertical div.) in this and all remaining figure parts. Windaq gain 8×. (f and g) Expanded and amplified (Windaq gain 32×) views of the evolution of I appearance after a J wave; f is expanded from box f in part showing J-I1 10 min after the end of J; g is stable J-I2 from 4.3 h later in this probe (not shown in part a).

Relative amplitudes of fine-structure H spikes were not appreciably different at Ri levels of 10^6 through 10^9 Ω (Figs. 1a and b and 2a–c), yet they were quite high and dominant in pathway at 10^{13} Ω (data not shown). At low Ri levels, H often appeared to alternate between low-amplitude high-frequency spikelet bursts and much lower-amplitude hump-like waves (Fig. 1b, first inset box; Table 1). At higher Ri levels, the waves disappeared and H was composed entirely of spikelets of varying low amplitudes and frequencies (Fig. 2d, inset box). Thus, spikes and spikelets were emf-dominated, whereas waves in humps were more R dominated because they were visible only at lower Ri levels. Also at very high Ri levels, H replaced G1 and sometimes also G2 at the start of each probe; G was diminished in amplitude (relative to its height at lower Ri levels) (Fig. 2a–c) or blended entirely with the then-larger spikes of H (10^{10} and 10^{13} Ω, not shown). It appeared that H itself was actually a complex underlying waveform that existed simultaneously with G during early pathway, but was masked by the overlying and much larger G at low Ri levels. Thus, H had a mixed electrical origin of both R and emf. Finally, at Ri 10^9 Ω or higher, the H waveform had a negative voltage level, thus was considered intracellular (Fig. 2a).

Family I. Waveform family I began abruptly after family H (or J waves; described later). I was a highly regular-frequency (6.5–9 Hz; Table 1) low-to-high amplitude waveform (depending upon Ri), occurring at varying voltage levels (Figs. 1a [H-I1, H-I2] and 2a [J-I1, J-I2]). The primary form of I was a series of monophasic, narrow, rounded or peaked square waves (termed rounded plateaus). Family I always began with waveform type I1, which was highly variable in amplitude, as well as number and shapes of the pla-

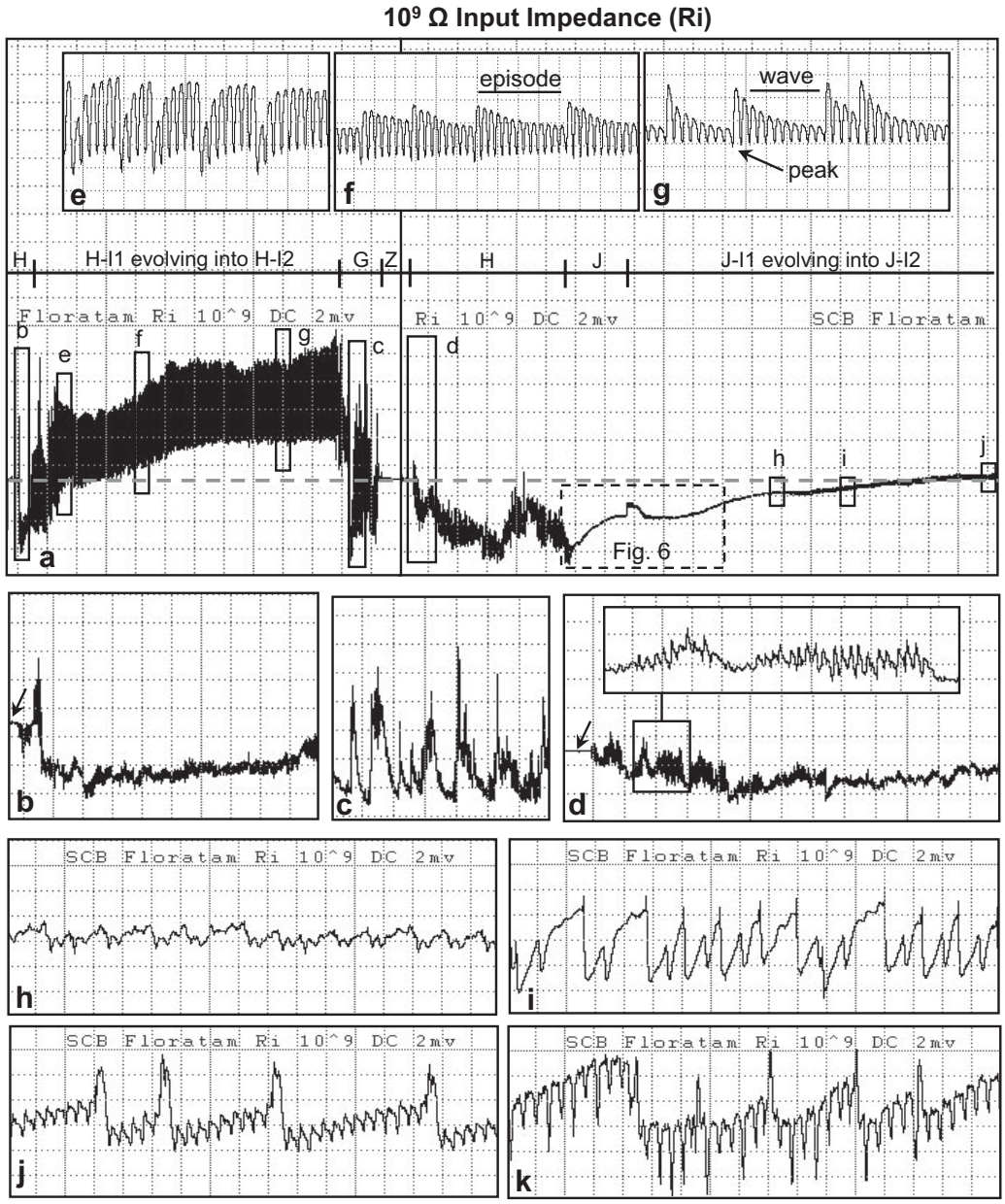

Fig. 2. Representative southern chinch bug waveforms using 2 mV DC applied signal and 10^9 Ω input impedance (Ri). (a) Compressed, side-by-side overview of the early parts of two typical probes. The first excerpt shows pathway H followed directly by putative ingestion (H-I), then a short return to G then Z (baseline, nonprobing [also known as NP]). The second excerpt shows mostly H followed by a J wave, then J-I1 that evolves into J-I2. Both probes show biphasic voltage levels, with the gray dashed line indicating the 0 V baseline level (see text for further discussion). Compression 300 (60 s/vertical div.), Windaq gain 8×. Boxes b, c, d, e, f, g, h, I, and j are expanded in their respective figure parts. (b–d) Expanded views of boxes b, c, and d in part a showing a few G2-like plateaus, but for the most part, very few details in pathway H other than the underlying 7–9 Hz-frequency wave, difficult to further categorize. Compression 13 (2.6 s/vertical div.), Windaq gain 8×. Unlabeled inset box in d shows expanded view to reveal the underlying 7–9 Hz-frequency wave. Compression 2 (0.40 s/vertical div.) in this and remaining figure parts. Windaq gain 8×. Arrow in part d denotes baseline/Z. (e–g) Expanded views of H-I waveforms in the same-lettered boxes in part a showing the evolution of putative I1 ingestion waveform appearance directly after H (Windaq gains 8×). Boxes e and f show H-I1, g is H-I2. (h–j) Expanded views of J-I waveforms in the same-lettered boxes in part a showing the evolution of putative ingestion waveform appearance directly after a J wave (Windaq gains 8× for h, 64× for i and j). Boxes h and i show J-I1; (j) shows J-I2. (k) J-I2 ingestion waveform, 2.2 h after part (j) (not shown on part a) (Windaq gain 64×).

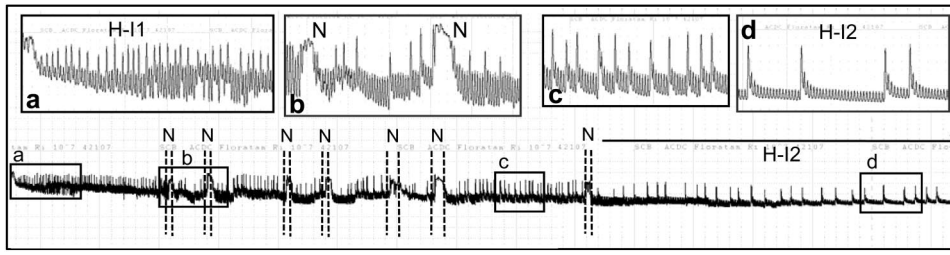

Fig. 3. Representative H-I waveforms of southern chinch bugs, using 10^7 Ω input impedance (Ri) and 0 V applied signal, showing complete evolution from H-I1 to H-I2 fine structure. Large outer figure box shows overview of 190 s of H-I, starting immediately after H. Vertical dotted lines delimit interruptions (waveform N). Boxes a, b, c, and d are expanded in their respective figure parts. Compression 10 (2.0 s/vertical div.), Windaq gain 16×. (a) Expanded view of box a, showing irregular peaks and waves of early H-I1. Compression 13 (2.6 s/vertical div.), Windaq gain 8×, in this and remaining figure parts. (b and c) Expanded views of boxes b and c showing development of regular peaks and waves during mid-H-I1 and (in box b) interruptions (N). (d) H-I2, with stable fine-structure that continued for another 174 s.

teaus (e.g., Fig. 1f). I1 evolved in appearance over time, transitioning through highly variable intermediate forms (e.g., Fig. 2e, f, h, and i). If the I waveform event lasted for more than a few seconds, repeated episodes of plateaus developed. The start of each episode was a single plateau (termed the "peak," Figs. 1e and 2g) that was higher in amplitude than any of the following plateaus within the episode (together termed the "wave," sometimes descending, as in Figs. 1e, g, and 2g, and sometimes ascending, as in Fig. 2j and k). Episodic peak-plus-wave fine-structure began to develop in mid-I1, eventually stabilizing at an appearance that remained constant (i.e., stereotypical amplitude and fine structure) within each Ri level for the rest of the event (Figs. 1g and 2g, j, and k). An entire sequence of this evolution is shown in Fig. 3. Once the waveform appearance became stable peaks-and-waves, it was termed I2. This "stable" I2 could continue, essentially unchanged, for many minutes to several hours (1–3 h of I was often seen in long southern chinch bug recordings).

I waveforms (including I1 transitional sequences that eventually stabilized as I2) could occur at two times during the stylet penetration sequence: 1) following pathway (usually after the first H event, although sometimes only a very short-duration stretch of H after G2), hereafter termed H-I1 or H-I2 sequences, or 2) following J (discussed below), hereafter termed J-I1 or J-I2 sequences. At all Ri levels, H-I2 events were 5–10× (or more) taller in absolute amplitude (Table 2) than J-I2 events (compare H-I vs J-I amplitudes in Figs. 1a and 2a). In addition, H-I waveform events (including both types I1 and I2) were always relatively short in duration (always <1 h) (Figs. 1a and 2a). In contrast, J-I events were very long in duration, usually exceeding 1 h, and often several hours long. Nonetheless, because episodes of both H-I and J-I were nearly identical in fine-structure appearance and frequency (Table 1), it was logical that all I waveforms should be named the same, regardless of their amplitude and the waveform that preceded them.

Of interest, voltage levels of H-I and J-I waveform events differed dramatically from one another at high Ri levels (10^9 Ω or higher). H-I sequences always occurred at a positive (considered "extracellular" at Ri 10^9 Ω) level, whereas J-I sequences always began at a negative (considered "intracellular" at Ri 10^9 Ω) level, and either continued negative or gradually drifted toward positive, to about the 0 V level or barely positive (Fig. 2a). Thus, I waveforms following H were distinctive in always being very large in absolute amplitude, short in duration, and at a positive extracellular voltage level at Ri 10^9 Ω; in contrast, I waveforms following J were always very short in amplitude, very long in duration, and at a negative intracellular voltage level at Ri 10^9 Ω.

In addition, relative amplitudes of peaks in H-I2 (the first plateau in each episode) decreased as the Ri level was increased. This finding was demonstrated by calculating the ratio of amplitudes of plateaus 1 (the peak) versus 3 (in the wave), at each Ri level. The 1:3 amplitude ratio significantly decreased with increasing Ri ($F = 3.61$; df = 4,24; $P = 0.0192$; Table 2; Fig. 4). As more plateaus occurred in the wave in each episode, their amplitudes increased relative to the height of the peak. Thus, the amplitude ratios of plateaus 1 versus 8 were not significantly different across Ri levels ($F = 1.22$; df = 4,24; $P = 0.3277$; Table 2; Fig. 4).

Table 2. Calculated peak ratios (means and SE) from H-I2 episodes at different Ri (input impedance) levels

Ri	N[a]	1:3 peak ratio	1:8 peak ratio
10^6 Ω	8	4.06 ± 0.78a	5.23 ± 1.26a
10^7 Ω	8	3.45 ± 0.70ab	3.54 ± 0.74a
10^8 Ω	8	3.38 ± 0.84ab	3.69 ± 1.13a
10^9 Ω	6	1.91 ± 0.43c	2.29 ± 0.73a
10^{10} Ω	8	2.59 ± 0.66bc	2.96 ± 0.88a
10^{13} Ω	2	0.99 ± 0.81	1.06 ± 0.87

Different lowercase letters indicate significant differences among ratios in each column, not including Ri 10^{13} Ω, for which the sample size was too small.

[a] N = number of insects from which one representative episode of stable H-I2 was measured. See Materials and Methods in text for details.

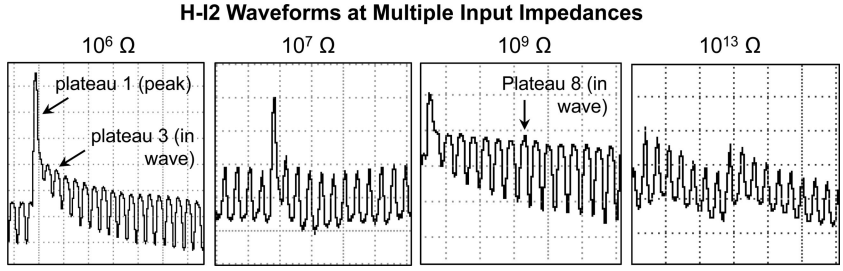

Fig. 4. Fine-structure waveform appearances of representative, stable H-I2 episodes of western and southern chinch bugs, at Ri levels of 10^6, 10^7, 10^9, and 10^{13} Ω, using DC applied signal.

Finally, H-I2 episodes had a slightly different appearance depending on whether an AC or a DC applied signal was used (Fig. 5). DC applied signal caused slight amplitude emphasis of the wave plateaus, whereas AC applied signal caused slight emphasis of the peak at low Ri levels (Fig. 5). Also, the peak at Ri 10^9 Ω and higher became intermittently biphasic, with both positive- and negative-going portions, for most insects (Figs. 2k and 5). The aforementioned electrical evidence supports that H-I2 had mixed electrical origins. The wave portion of each I2 episode was primarily emf component, whereas the peak was more R-dominated at lower Ri levels, until Ri levels of 10^9 Ω or higher, when emf (especially the negative-going, biphasic peak; Fig. 2e and k) co-occurred with R.

Family J. An abrupt transition in waveform appearance often occurred at the end of waveform fam-

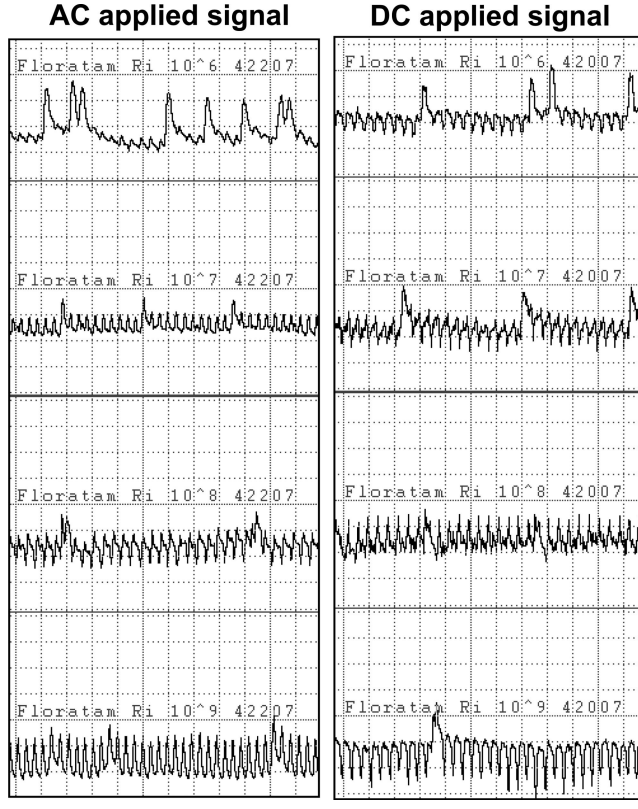

Fig. 5. Comparison of stable J-I2 waveforms from four different southern chinch bugs recorded simultaneously at four Ri levels (10^6, 10^7, 10^8, and 10^9 Ω; note user annotations in traces). All four recordings were started with AC applied signal; recording was first captured at ≈2.8 h after start of recording (left column) and 2.5 h after recording the J wave for the insect in channel 1. Insects on the other three channels had been ingesting since the start of recording. At 11.3 h after the start of recording, the applied signal was switched to DC. Recording was captured again (right column) at 15.5 h after the start of recording, when all four insects had achieved sustained J-I2 in subsequent probes at 2, 4.8, 1.1, and 3.0 h, after previously recorded J waves. Compression 2 (0.40 s/div.), AC Windaq gains were 128× for all Ri levels, except 10^9 Ω, which was 64×; DC Windaq gains were 64× for Ri 10^6 and 10^7 Ω, and 128× for Ri levels 10^8 and 10^9 Ω.

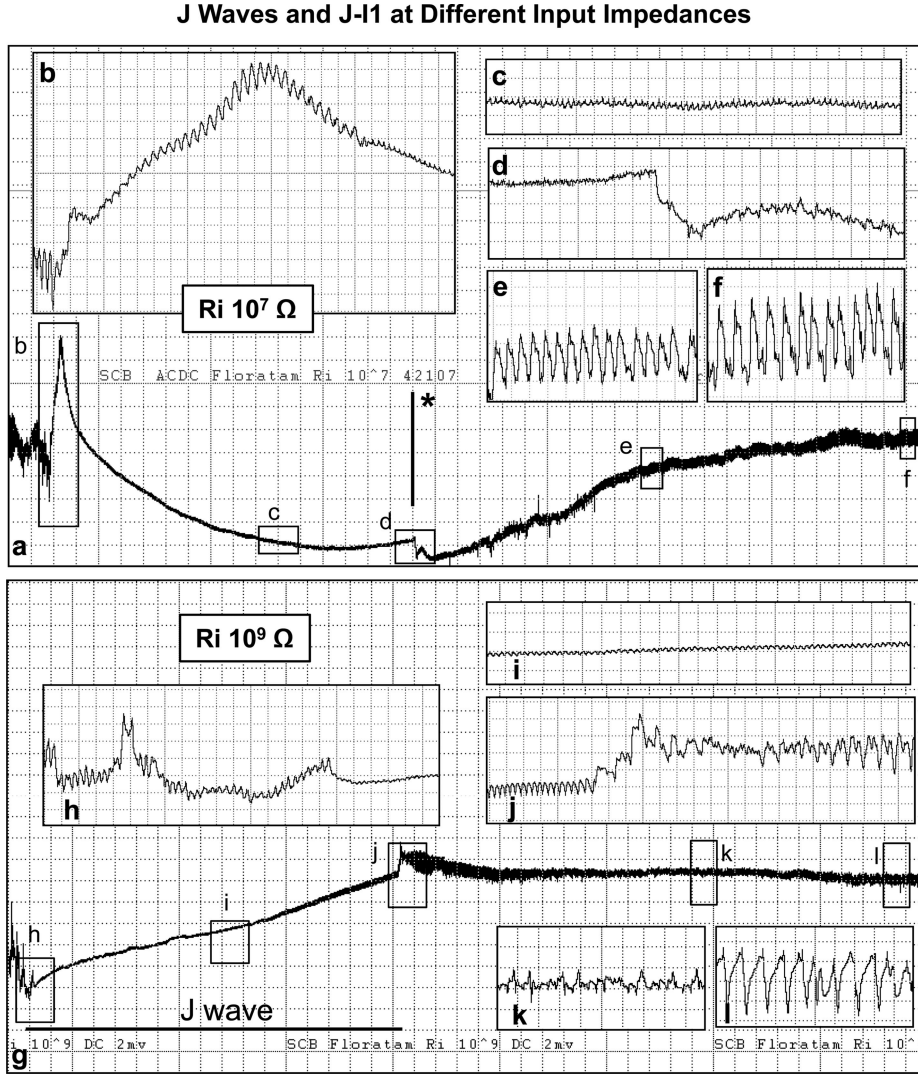

Fig. 6. Southern chinch bug J waves. (a) Moderately expanded view of J wave and subsequent, evolving J-I1 waveform at Ri 10^7 Ω. Boxes b, c, d, e, and f are expanded in their respective figure parts. Vertical bar with asterisk marks end of J wave with small but abrupt voltage drop. Compression 50 (10 s/vertical div.), Windaq gain 32×. (b–f). Expanded views of boxes b, c, d, e, and f in part a. Compression 2 (0.40 s/vertical div.), Windaq gains 64× for (b), 128× for (c–f). (g) Moderately expanded view of J wave and subsequent, evolving J-I1 waveform at Ri 10^9 Ω. Boxes h, i, j, k, and l are expanded in their respective figure parts. Compression 50 (10 s/vertical div.), Windaq gain 4×. (h–l) Expanded views of boxes h, i, j, k, and l in part g. Compression 2 (0.40 s/vertical div.), Windaq gains 16× for (h–j), 32× for (k and l).

ily H, often after a sequence of H →I →H events. At low Ri levels of 10^6 to 10^7 Ω, sometimes also 10^8 Ω, a medium-amplitude positive-going rise in voltage occurred. This rise was then followed by a complex stereotypically repeating waveform (termed a J wave). The overlying medium-structure waveform consisted of a rapid positive slope to a medium-height, distinct, rounded peak (Fig. 6a and b), followed by a relatively long negative-going slope (Fig. 6a and c), down to an abrupt end at a small voltage drop (Fig. 6a [*] and d). A much smaller underlying waveform also occurred, whose fine structure was a low-amplitude, highly regular-frequency (9–12 Hz), peaked sine wave superimposed on the medium structure (Fig. 6b and c). We define a single episode of J wave as the duration from the voltage rise to the abrupt voltage drop (Fig. 6a and d); usually there were one or two episodes (Fig. 1a) before commencement of J-I1, not more than two.

The overlying medium structure of the J wave was present with the same appearance (neither increasing nor decreasing in amplitude) at all Ri levels from 10^6 to 10^{10} Ω. At low Ri levels, where the general voltage level was monophasic, the overlying medium structure of the J wave was positive-going (Fig. 6a). However, at Ri 10^9 Ω and higher (and

sometimes also at Ri 10^8 Ω), when the general voltage level of the total recording became biphasic, the J wave inverted (Fig. 6g, h and j). The voltage drop at the end of the J wave also inverted, becoming a voltage rise. Yet the underlying, fine-structure, short sine wave did not invert; it always remained positive-going at all Ri levels. Interestingly, at Ri 10^{13} Ω, the overlying medium-structure curve of the J wave disappeared entirely, leaving only the underlying fine-structure sine wave that ended at a still-present voltage drop. The aforementioned results indicate that the J wave medium-structure curve is primarily R component. In contrast, the overlying fine-structure sine wave is dominated by emf, and the voltage change at the end is both R and emf. Thus, the electrical origin of the J wave was a mixture of R and emf.

Following the J wave, a highly variable but evolving J-I1 waveform always occurred. Its underlying fine structure began as a semi-regular (6.5–9 Hz), short, highly peaked square wave (Fig. 6e), gradually becoming more organized into plateaus that slowly grew in amplitude and became more upwardly pointed with time. The evolution of this regular waveform was elaborate and required many seconds to several minutes (Fig. 6e, f, j, k, and l). However, over time, the waveform came to resemble the same I1 as typically followed H. The overlying medium structure was a gradual slope upward, eventually plateauing to a more-or-less level constant-amplitude waveform (Fig. 6a). Thus, the erratic but regular fine structure of the immediate post-J I1 waveform evolved into appearances similar to H-I1 (compare Fig. 6k and l with Fig. 2h and i), which within a few minutes evolved into typical I2 waveform (similar to Fig. 2j and k). Consequently, all I waveforms following the late-J wave voltage change are termed J-I1 evolving into J-I2 (Table 1).

Family N. During H-I1 waveform, it was common for short irregular interruptions of the waveform to occur. These interruptions, termed waveform family N, took the form of an abrupt voltage rise, spikey leveling, then sudden voltage drop, resulting in a short-duration (a few seconds), wide, flat-spikey plateau (Fig. 3a and b). The voltage rise was typically to the same level as the nearby evolving H-I1 peaks (Fig. 3). N interruptions always occurred during H-I1, before reaching the waveform appearance reaching stability in I2; they were never seen in J-I1. Interestingly, the N plateau was always positive-going at low Ri levels (10^6 and 10^7 Ω), negative-going with larger more detailed spikes at the bottom at high Ri levels (10^9, 10^{10}, and 10^{13} Ω), and either positive- or negative-going at 10^8 Ω.

Discussion

Whenever new insect species (such as the present two chinch bugs) are recorded for the first time with EPG, a consistent series of experiments must be performed to first identify and describe (termed "characterize") the researcher-identified waveforms, and then to determine their biological meanings (termed "correlate"). These experiments comprise the "triangle of correlations" (Walker 2000) to define the waveform via the insect's stylet activities (i.e., salivation, ingestion, stylet movements) and stylet tip location in the plant (e.g., mesophyll, phloem sieve elements, or xylem). The correlation process can be long and arduous, often requiring years of highly specialized methodology, such as plant histology and light, confocal, or electron microscopy; excretory droplet studies; electromyography; and other methods (Walker 2000). Nonetheless, only after such work can the waveforms be definitively defined and EPG knowledgably used as a tool for further studies. One of the largest challenges facing EPG science today is the pressing call to quickly adapt and use EPG as a tool for urgently needed studies of insect feeding; this is especially true for exotic and invasive hemipteran pest species. These days, however, there often is limited time or funding for the full, labor-intensive, and time-consuming waveform correlation process.

The current study is an attempt to provide alternative methods to partially shorten the lengthy waveform correlation and definition process. Our work builds on techniques developed over the past 40 yr of EPG science (Tjallingii 1985, Backus 1994, Walker 2000), but also uses novel capabilities of the new AC–DC monitor (Backus and Bennett 2009), especially its flexible input resistor/impedance [Ri] switches. Our objective was to learn enough about the electrical properties of chinch bug waveforms to hypothesize some important biological meanings for waveforms, before completing the triangle of correlations. We also sought to develop experiments that could become standards for future studies of the electrical nature of waveforms. The current study is not to suggest that electrical methods can, or should, supplant traditional correlations. Completing the full triangle of correlation experiments for each new insect group is of great importance. However, sometimes such tests can be exceptionally difficult to perform, as was the case with chinch bugs.

Although chinch bugs make salivary sheaths, sometimes quite elaborate ones (Anderson et al. 2006, Rangasamy et al. 2009), they do so through the tightly wrapped immature leaf sheaths in grass blades. Thus, each salivary sheath traverses multiple young leaves separated by layers of air space. We made numerous attempts to mark, excise leaf sheath tissues, and histologically prepare salivary sheaths from correlated EPG waveforms. However, the loosely wrapped leaf sheaths often fell apart, or salivary sheaths tore, during processing. In addition, we could not collect uncontaminated excretory droplets, because chinch bugs prefer to lodge their bodies tightly between the leaf sheaths and excrete within the tight space they make. Consequently, we sought to thoroughly characterize EPG waveforms for chinch bugs, and then to use electrical experiments to hypothesize the

putative biological meanings of these waveforms, sufficient to support tentative conclusions for future quantitative comparisons of resistant and susceptible host plants.

The current study carefully described and characterized for the first time the EPG waveforms of two related species of chinch bugs (Heteroptera: Blissidae) and performed a rigorous study of the electrical origins of their waveforms. EPG studies of numerous hemipteran species over the past 30 yr have allowed development of strong theoretical underpinnings to describe the electrical origins (termed R and emf components) of EPG waveforms (Tjallingii 1978, 1985; Walker 2000; Backus and Bennett 2009). Of particular importance is understanding the R-emf responsiveness curve (Backus and Bennett 2009), as well as the biological basis of R and emf components. Information on the electrical origin of waveforms was combined with similarities in appearance between chinch bug waveforms and other species (aphids and several leafhopper species such as sharpshooters). The result allowed us to hypothesize the following putative waveform definitions and biological meanings for chinch bug waveforms. These hypotheses can be tested in future correlation studies.

Pathway Waveforms, G and H. The earliest waveforms in stylet penetration undoubtedly represent formation of the salivary sheath as stylets penetrate to a preferred ingestion tissue (termed pathway activities), as has been demonstrated with all other recorded salivary sheath feeders. Because saliva is highly electrically conductive, waveforms derived primarily from salivation are heavily R-dominated. Chinch bug G2 strongly resembled the A1 salivation peaks of sharpshooter leafhoppers (Backus et al. 2005), which have been electrically and histologically correlated with salivation of the sheath flange and trunk, as well as stylet advancement. Similarly, chinch bug H resembles the sharpshooter B1 waveform, which has been histologically correlated with stylet progression, narrow sheath branch formation, and deep penetration to the vascular bundle. Both A1 and B1 in sharpshooters are primarily R-component waveforms, similar to G and H in chinch bug recordings.

Putative Ingestion Waveform, I. All I waveforms have both R and emf origins; however, the most regular wave-like portions are emf-dominated, probably because of streaming potentials caused by fluid (either saliva or food) pumping. Chinch bug I1 sometimes resembles the E1 waveform of aphids (Prado and Tjallingii 1994), especially at Ri of 10^9 Ω. Therefore, I1 may represent salivation into a phloem cell, with or without simultaneous passive ingestion. I1 evolves into I2 (regardless of whether preceded by H or J), whose peak-and-wave structure resembles the ingestion waveform of corn leafhoppers, *Dalbulus maidis* Wolcott (Carpane et al. 2011). This peak-and-wave structure suggests active ingestion, that is, cibarial pumping of sap food. Dugravot et al. (2008) determined that the amplitude of sharpshooter ingestion plateaus was proportional to the degree of uplift of the cibarial diaphragm. Thus, for each I2 episode, perhaps waves represent multiple cibarial pumps, each partially filling the cibarium (Dugravot et al. 2008), with peaks possibly representing complete opening and filling of the cibarium. Alternatively, the peak could represent closure of either the cibarial diaphragm or the precibarial valve (blocking the precibarium, therefore causing resistance to electrical flow, that is, R), to swallow fluid down the pharynx (Dugravot et al. 2008). In a third alternative, I2 peaks may represent a brief spurt of salivation into a vascular cell. It is also possible that the higher amplitude of H-I waveforms, compared with J-I waveforms, means that greater suction is generated during cibarial pumping in H-I versus J-I.

Putative Phloem Contact, the J Wave. The J wave is a unique apparently species-specific waveform that does not resemble any waveform previously published from any other EPG-recorded species. Such a unique appearance is typical of an X wave, an early concept in EPG science (McLean and Kinsey 1967) that recently has been updated (Backus et al. 2009). According to that recent article, an X wave is "a multi-component waveform family representing multiple stylet activities that comprise tasting and testing of a possible preferred ingestion cell; when preceding an ingestion waveform, (an X wave) indicates [that subsequent] ingestion is from a preferred cell type such as phloem (aphids, leafhoppers) or xylem (sharpshooters)." Accordingly, we propose that the chinch bug J wave is analogous to the X waves of aphids and leafhoppers. X waves are hypothesized to represent simultaneous precibarial valve and cibarial diaphragm movements controlling minute fluid uptake and egestion, combined with salivation (Backus et al. 2009). As an ecological concept, the X wave phase represents the complex process of accepting a potential ingestion cell, analogous to acceptance of a host plant. Thus, the X wave is a marker for ecologically important foraging behaviors, in any hemipteran.

We propose that the overlying medium-structure curve of the J wave, highly R-dominated, represents the stylet tips pushing against the cell wall and/or membrane of a phloem sieve element, with the abrupt voltage change at the end representing the tips breaking through. Unlike for aphids, this membrane breakage is due to a mixture of R and emf, probably because the large stylets of chinch bugs partially destroy (rather than retain, as in aphids) the charge separation of the cell membrane. The underlying, fine-structure, emf-dominated sine wave may represent salivation that begins as the stylets are pushed into the cell and continues within the phloem cell, analogous to aphid E1 phloem salivation.

Putative Xylem- and Phloem-Ingestion Waveforms, H-I and J-I, Respectively. Given that chinch bugs are considered predominantly phloem-ingesting species (and assuming that our J-wave-equals-X-wave hypothesis proves true, after future correlation studies), it follows that J-I2 sequences may represent ingestion from phloem sieve elements and H-I2 sequences may

represent ingestion from xylem tracheary elements. This hypothesis is strongly supported by the electrical findings in this article, especially that H-I is characterized by: 1) positive, extracellular voltage level (characteristic for xylem ingestion waveforms in aphids and sharpshooters), 2) high absolute amplitude suggesting higher cibarial diaphragm uplift required to pump high-tension xylem fluid, and 3) short durations of H-I sequences early in a probe (suggesting slaking of "thirst" after dehydration during wiring). Similarly, J-I is characterized by 1) negative intracellular voltage level (characteristic for phloem-ingestion waveforms); 2) very low absolute amplitude (suggesting minor cibarial uplift for barely-active, mostly passive ingestion); and 3) very long durations of J-I sequences, later in the probe.

Putative Salivation Into and/or Tasting of Xylem Cells During N. Broad plateau-like interruptions occurred in early H-I1 waveforms, which strongly resemble similar interruptions during sharpshooter recordings of xylem ingestion. Sharpshooter N waveforms are, like chinch bug N, positive-going at low Ri levels, but negative-going at high Ri levels (Backus et al. 2005, 2009). Histological correlations have found that sharpshooter interruptions represent sheath salivation into and putative tasting of xylem cells (Backus et al. 2012). We propose a similar biological meaning for interruptions in chinch bugs. The absence of N waveforms following J supports that J-I1 may be the sole form of salivation in phloem cells.

The aforementioned hypothesized biological meanings of chinch bug waveforms will be useful for tentative interpretations of quantitative studies comparing chinch bug feeding on different host plants. Such a study, comparing southern chinch bug feeding on resistant and susceptible St. Augustinegrass, has been performed (Rangasamy 2008). Waveform quantification has not been performed with data from the current study, because that has been done in the quantitative study.

Based on the results of the electrical experiments described herein, it is recommended that future EPG studies of chinch bug feeding use 10^7 Ω as the standard amplifier sensitivity (input impedance, or Ri). Ri of 10^7 Ω provided the clearest visualization of all waveform phases, families, and types for chinch bugs. This was not the case for Ri of 10^6 Ω, which often distorted or eliminated emf-dominated waveforms such as I, or 10^9 Ω and higher, which distorted or obscured R-dominated pathway waveforms such as G. Either AC or DC applied signals can be used, as neither appeared to disturb the insects or reduce the information value of the waveforms recorded. (It should be noted, however, that very low voltage levels were deliberately chosen for this study. A few preliminary observations suggested that higher voltages [>100 mV] of DC combined with low Ri levels [therefore creating high current densities in the insect] caused chinch bugs to cease probing.) As long as applied voltages are low, researchers can choose whichever applied signal type leads to the least noise in their environment. We also recommend use of gold wire of diameter 25 μm instead of 12.7 μm, and use of silver glue instead of silver paint, for more consistent wiring quality.

The present work characterized the EPG waveforms for two species of chinch bug, western and southern, and found that they were similar. In addition, the current study provided electrical evidence for hypothesized biological meanings for all of the chinch bug waveforms, including putative phloem and xylem sap ingestion. Evidence provisionally supports the conclusion that chinch bugs are salivary sheath feeders that are capable of ingesting from both xylem tracheary and phloem sieve elements, but preferentially from phloem cells. In the current study, chinch bugs performed a rather stereotypical series of behaviors during stylet probing, starting with putative pathway activities (formation of a salivary sheath), progressing to short events of putative xylem ingestion, followed by a return to sheath formation, and then an X wave-like transition to phloem ingestion for variable long durations. Further quantification of chinch bug feeding, on both susceptible and resistant genotypes, will be possible now that the present waveform characterization has been accomplished.

Acknowledgments

We thank Holly Shugart and Jose Gutierrez (U.S. Department of Agriculture–Agriculture Research Service) for their help during the EPG Workshop at California State University, Fresno, in 2005, and for numerous subsequent attempts to collect excretory droplets and perform plant histological correlations for southern chinch bug waveforms. We thank Russell Nagata (UF/IFAS, Everglades Research and Education Center) for supplying St. Augustinegrass. This research was supported by a Wedgworth fellowship (to M.R.) and the Florida Agricultural Experiment Station.

References Cited

Almeida, R.P.P., and E. A. Backus. 2004. Stylet penetration behaviors of *Graphocephala atropunctata* (Signoret) (Hemiptera, Cicadellidae): EPG waveform characterization and quantification. Ann. Entomol. Soc. Am. 97: 838–851.

Anderson, W. G., T. M. Heng–Moss, and F. P. Baxendale. 2006. Evaluation of cool- and warm-season grasses for resistance to multiple chinch bug (Hemiptera: Blissidae) species. J. Econ. Entomol. 99: 203–211.

Backus, E. A. 1994. History, development, and applications of the AC electronic monitoring system for insect feeding, pp. 1–51. *In* M. M. Ellsbury, E. A. Backus, and D. L. Ullman (eds.), History, Development, and Application of AC Electronic Insect Feeding Monitors. Entomological Society of America, Lanham, MD.

Backus, E. A., and W. H. Bennett. 1992. New AC electronic insect feeding monitor for fine-structure analysis of waveforms. Ann. Entomol. Soc. Am. 85: 437–444.

Backus, E. A., and W. H. Bennett. 2009. The AC-DC correlation monitor: new EPG design with flexible input resistors to detect both R and emf components for any piercing-sucking hemipteran. J. Insect Physiol. 55: 869–884.

Backus, E. A., M. J. Devaney, and W. H. Bennett. 2000. Comparison of signal processing circuits among seven AC electronic monitoring systems for their effects on the emf and R components of aphid (Homoptera: Aphididae) waveforms, pp. 102–143. *In* G. P. Walker and E. A. Backus (eds.), Principles and Applications of Electronic Monitoring and Other Techniques in the Study of Homopteran Feeding Behavior. Entomological Society of America, Lanham, MD.

Backus, E. A., J. Habibi, F. Yan, and M. Ellersieck. 2005. Stylet penetration by adult *Homalodisca coagulata* on grape: electrical penetration graph waveform characterization, tissue correlation, and possible implications for transmission of *Xylella fastidiosa.* Ann. Entomol. Soc. Am. 98: 787–813.

Backus, E. A., A. R. Cline, M. R. Ellerseick, and M. S. Serrano. 2007. *Lygus hesperus* (Hemiptera: Miridae) feeding on cotton: new methods and parameters for analysis of nonsequential electrical penetration graph data. Ann. Entomol. Soc. Am. 100: 296–310.

Backus, E. A., W. J. Holmes, F. Schreiber, B. J. Reardon, and G. P. Walker. 2009. Sharpshooter X wave: Correlation of an electrical penetration graph waveform with xylem penetration supports a hypothesized mechanism for *Xylella fastidiosa* inoculation. Ann. Entomol. Soc. Am. 102: 847–867.

Backus, E. A., K. B. Andrews, H. J. Shugart, L. Carl Greve, J. M. Labavitch, and H. Alhaddad. 2012. Salivary enzymes are injected into xylem by the glassy-winged sharpshooter, a vector of *Xylella fastidiosa.* J. Insect Physiol. 58: 949–959.

Baxendale, F. P., T. M. Heng–Moss, and T. P. Riordan. 1999. *Blissus occiduus* (Hemiptera: Lygaeidae): a chinch bug pest new to buffalograss turf. J. Econ. Entomol. 92: 1172–1176.

Bonjour, E. L., W. S. Fargo, J. A. Webster, P. E. Richardson, and G. H. Brusewitz. 1991. Probing behavior comparisons of squash bugs (Heteroptera: Coreidae) on cucurbit hosts. Environ. Entomol. 20: 143–149.

Carpane, P., A. Wayadande, E. Backus, W. Dolezal, and J. Fletcher. 2011. Characterization and correlation of new electrical penetration graph waveforms for the corn leafhopper (Hemiptera: Cicadellidae). Ann. Entomol. Soc. Am. 104: 515–525.

Cherry, R. 2001. Seasonal wing polymorphism in southern chinch bugs (Hemiptera: Lygaeidae). Fla. Entomol. 84: 737–739.

Cline, A. R., and E. A. Backus. 2002. Correlations among AC electronic monitoring waveforms, body postures, and stylet penetration behaviors of *Lygus hesperus* (Hemiptera: Miridae). Environ. Entomol. 31: 538–549.

Cook, C. A., and J. J. Neal. 1999. Feeding behavior of larvae of *Anasa tristis* (Heteroptera: Coreidae) on pumpkin and cucumber. Environ. Entomol. 28: 173–177.

Crocker, R. L., R. W. Toler, J. B. Beard, M. C. Engelke, and J. S. Kubicabreier. 1989. St. Augustinegrass antibiosis to southern chinch bug (Hemiptera, Lygaeidae) and to St. Augustinegrass decline strain of *Panicum* mosaic virus. J. Econ. Entomol. 82: 1729–1732.

Dugravot, S., E. A. Backus, B. J. Reardon, and T. A. Miller. 2008. Correlations of cibarial muscle activities of *Homalodisca* spp. sharpshooters (Hemiptera: Cicadellidae) with EPG ingestion waveform and excretion. J. Insect Physiol. 54: 1467–1478.

Eickhoff, T. E., F. P. Baxendale, T. M. Heng–Moss, and E. E. Blankenship. 2004. Turfgrass, crop, and weed hosts of *Blissus occiduus* (Hemiptera: Lygaeidae). J. Econ. Entomol. 97: 67–73.

Eickhoff, T. E., F. P. Baxendale, and T. M. Heng–Moss. 2006. Host preference of the chinch bug, *Blissus occiduus.* J. Insect Sci. 6: 6. (insectscience.org/6.07).

Eickhoff, T. E., T. M. Heng–Moss, F. P. Baxendale, and J. E. Foster. 2008. Levels of tolerance, antibiosis, and antixenosis among resistant buffalograsses and zoysiagrasses. J. Econ. Entomol. 101: 533–540.

Heng–Moss, T. M., F. P. Baxendale, T. P. Riordan, and J. E. Foster. 2002. Evaluation of buffalograss germplasm for resistance to *Blissus occiduus* (Hemiptera: Lygaeidae). J. Econ. Entomol. 95: 1054–1058.

Heng–Moss, T. M., F. P. Baxendale, T. P. Riordan, L. Young, and K. Lee. 2003. Chinch bug-resistant buffalograss: an investigation of tolerance, antixenosis, and antibiosis. J. Econ. Entomol. 96: 1942–1951.

Kerr, S. H. 1966. Biology of the lawn chinch bug, *Blissus insularis.* Fla. Entomol. 49: 9–18.

McLean, D. L., and M. G. Kinsey. 1964. A technique for electronically recording aphid feeding and salivation. Nature 202: 1358–1359.

McLean, D. L., and M. G. Kinsey. 1967. Probing behavior of the pea aphid, *Acyrthosiphon pisum.* I. Definitive correlation of electronically recorded waveforms with aphid probing activities. Ann. Enomol. Soc. Am. 60: 400–405.

Painter, R. H. 1928. Notes on the injury to plant cells by chinch bug feeding. Ann. Entomol. Soc. Am. 21: 232–242.

Prado, E., and W. F. Tjallingii. 1994. Aphid activities during sieve element punctures. Entomol. Exp. Appl. 72: 157–165.

Rangasamy, M. 2008. Mechanisms of resistance to southern chinch bug, Blissus insularis Barber (Hemiptera: Blissidae), in St. Augustinegrass. Ph.D. dissertation, University of Florida, Florida.

Rangasamy, M., H. J. McAuslane, R. H. Cherry, and R. T. Nagata. 2006. Categories of resistance in St. Augustinegrass lines to southern chinch bug (Hemiptera: Blissidae). J. Econ. Entomol. 99: 1446–1451.

Rangasamy, M., B. Rathinasabapathi, H. J. McAuslane, R. H. Cherry, and R. T. Nagata. 2009. Role of leaf sheath lignification and anatomy in resistance against southern chinch bug (Hemiptera: Blissidae) in St. Augustinegrass. J. Econ. Entomol. 102: 432–439.

Reinert, J. A., and S. H. Kerr. 1973. Bionomics and control of lawn chinch bugs. Bull. Entomol. Soc. Am. 19: 91–92.

Reinert, J. A., P. Busey, and F. G. Bilz. 1986. Old World St. Augustine grasses resistant to the southern chinch bug (Heteroptera, Lygaeidae). J. Econ. Entomol. 79: 1073–1075.

Reinert, J. A., A. Chandra, and M. C. Engelke. 2011. Susceptibility of genera and cultivars to southern chinch bug *Blissus insularis* (Hemiptera: Blissidae). Fla. Entomol. 94: 158–163.

SAS Institute. 2001. PROC user's manual, version 6th ed. SAS Institute, Cary, NC.

Slater, J. A. 1976. Monocots and chinch bugs: a study of host plant relationships in the lygaeid subfamily blissinae (Hemiptera: Lygaeidae). Biotropica 8: 143–165.

Tjallingii, W. F. 1978. Electronic recording of penetration behaviour by aphids. Entomol. Exp. Appl. 24: 721–730.

Tjallingii, W. F. 1985. Electrical nature of recorded signals during stylet penetration by aphids. Entomol. Exp. Appl. 38: 177–186.

van Helden, M., and W. F. Tjallingii. 2000. Experimental design and analysis in EPG experiments with emphasis on plant resistance research, pp. 144–171. *In* G. P. Walker

and E. A. Backus (eds.), Principles and Applications of Electronic Monitoring and Other Techniques in the Study of Homopteran Feeding Behavior. Thomas Say Publications in Entomology. Entomological Society of America, Lanham, MD.

Vittum, P. J., M. G. Villani, and H. Tashiro. 1999. Turfgrass insects of the United States and Canada. Cornell University Press, Ithaca, NY.

Walker, G. P. 2000. Beginner's guide to electronic monitoring, pp. 14–40. *In* G. P. Walker and E. A. Backus (eds.), Principles and Applications of Electronic Monitoring and Other Techniques in the Study of Homopteran Feeding Behavior. Entomological Society of America, Lanham, MD.

Received 12 February 2013; accepted 31 May 2013.